# Numerical simulation of optical feedback on a quantum dot lasers

© *Amin H. Al-Khursan* [¶], *Basim Abdullattif Ghalib* [∗], *Sabri J. Al-Obaidi* [∗∗]

Nassiriya Nanotechnology Research Laboratory (NNRL), Science College, Thi-Qar University,
Nassiriya, Iraq
[∗] Laser Physics Department, Science College for Women, Babylon University,
Hilla, Iraq
[∗∗] Physics Department, Science College, Al-Mustansiriyah University,
Baghdad, Iraq

We use multi-population rate equations model to study feedback oscillations in the quantum dot laser. This model takes into account all peculiar characteristics in the quantum dots such as inhomogeneous broadening of the gain spectrum, the presence of the excited states on the quantum dot and the non-confined states due to the presence of wetting layer and the barrier. The contribution of quantum dot groups, which cannot follow by other models, is simulated. The results obtained from this model show the feedback oscillations, the periodic oscillations which evolves to chaos at higher injection current of higher feedback levels. The frequency fluctuation is attributed mainly to wetting layer with a considerable contribution from excited states. The simulation shows that is must be not using simple rate equation models to express quantum dots working at excited state transition.

## 1. Introduction

Quantum dot (QD) semiconductor lasers and amplifiers get an increasing interest in the last and this decades due to their interesting properties adequate for telecommunication applications. These properties includes low sensitivity to optical feedback resulting from „relatively low" linewidth enhancement factor (LEF) and strong damping of relaxation oscillations [1,2]. Although the low sensitivity is required for some applications, the high sensitivity is required in others like chaos communications where many types of dynamic behavior are possible [3,4]. Thus, the demand property is the controllable sensitivity to optical feedback. A strong optical feedback induces an instabilities in QDs very different from those commonly observed in quantum well lasers and cannot be explained in the frame of the conventional Lang and Kobayashi theory [5] because experimental conditions include high pumping current, strong optical feedback, and a relatively long external cavity. Analysis of rate equation models for external cavity lasers has shown that the LEF, the laser relaxation oscillations, and the external cavity round-trip time are important parameters for the appearance of these instabilities [3]. All the analysis of feedback in QD lasers is done depending of the simple rate equation (SRE) models to formulate processes of carriers into the dots. This results in a deviations from experimental data since the measured LEF in QD lasers depends significantly on the measurement procedure: the above threshold measured LEF depends on the carrier filling and on the dynamics in the QD states that don't contribute to the stimulated emission process but it increases with the unjection current [6]. Consequently the measured LEF above threshold is different from the one measured at threshold and depends on the operation conditions. This behavior is the direct consequence of the complexity of the QD material: the non uniformity of QD dimensions, presence of the wetting layer (WL), in addition to several confined states in the

QDs determined by the self assembling growth process causes an inhomogeneous broadening, asymmetry of the gain spectrum and affects the chirp. This makes the carrier and photon dynamics cannot be approximated, as in bulk or quantum well case, with a standard SREs system. According to this, QD layer must be sub-grouped according to the homogenous broadening. This is done through the multi-population rate equations (MPRE) model as introduced in [7].

Regarding the SRE models, the inclusion of special characteristics of QDs in the rate equation models to study optical feedback is still missing. Here we use MPRE model coupled with the field equation to simulate QD laser with optical feedback. Attention is paid to parameters like injection current and external cavity round-trip time. This paper is organized as follows: in section 2, the MPRE model with optical feedback is introduced. Choice of operating point and then feedback behavior using MPRE model is calculated and discussed in section 3 before concluding in section 4.

## 2. MPRE model with optical feedback

In the MPRE model the effects of many QD groups including ground- and excited states (GS and ES), WL states and the separate confinement heterostructure (SCH) barrier layer, the carrier processes in and out of the dots, the refractive index variation expressed by the linewidth enhancement factor, LEF, and the chirp results from the contributions of QD and plasma effects are taken into account. The effect of size fluctuation of QDs is included by dividing the QD ensemble into several sub-groups each characterized by an average energy of the excited state, $E_{ESm}$, and of the ground state, $E_{GSm}$, respectively. The temporal evolution due to the round-trip in the external cavity is included in the equation of the electric field which is coupled to MPRE. Then, the MPRE model with optical

[¶] E-mail: ameen_2all@yahoo.com

feedback is as follows:

$$\frac{de_{GS}}{dt} = \beta \frac{N_{GS}}{\tau_r} + \frac{c\Gamma}{n_r} \sum_j (g_{jmGS})e_{GS} - \frac{e_{GS}}{\tau_{pGSm}}$$
$$+ i\delta\omega e_{GS} + \frac{\gamma}{2} e_{GS}(t - \tau_{delayed}), \qquad (1)$$

$$\frac{dN_s}{dt} = \frac{I}{q} - \frac{N_s}{\tau_s} - \frac{N_s}{\tau_{sr}} + \frac{N_{wl}}{\tau_{we}}, \qquad (2)$$

$$\frac{dN_{wl}}{dt} = \frac{N_s}{\tau_s} - \frac{N_{wl}}{\tau_{wr}} - \frac{N_{wl}}{\tau_{we}}$$
$$+ \sum_m \frac{N_{eESm}}{\tau_{eESm}} - \frac{N_{wl}}{\tau_{c0}} \sum_m (1 - P_{ESm})G_m \qquad (3)$$

$$\frac{dN_{ESm}}{dt} = \frac{N_{wl}G_m(1 - P_{EGm})}{\tau_{c0}} + \frac{N_{GSm}(1 - P_{ESm})}{\tau_{eGSm}} - \frac{N_{ESm}}{\tau_r}$$
$$- \frac{N_{ESm}}{\tau_{eESm}} - \frac{N_{ESm}}{\tau_{d0}}(1 - P_{GSm}), \quad m = 0, 1, \dots, M-1, \quad (4)$$

$$\frac{dN_{GSm}}{dt} = \frac{N_{ESm}}{\tau_{d0}}(1 - P_{GSm}) - \frac{N_{GSm}}{\tau_r} - \frac{N_{GSm}(1 - P_{DESm})}{\tau_{eGSm}}$$
$$- \frac{c\Gamma}{n_r} \sum_j g_{jmGS}|e_{GS}|^2 \qquad m = 0, 1, \dots, M-1. \qquad (5)$$

In the system Eqs (1)–(5), $N_s$ and $N_{wl}$ are not total number of carriers in the SCH and the WL, $N_{ESm}$ and $N_{GSm}$ are the carrier number in the $m^{th}$-ES and $m^{th}$-GS, respectively; $e_{GS}$ is the complex amplitude of the electric field due to the GS transition. Since the behavior analyzed here is for a single longitudinal mode laser, so only one rate equation for the electric field is considered. It is assumed here that the laser emits with average GS mode. This is possible since the laser is a distributed Bragg reflector (DBR) laser. The laser mode of DBR chosen at the GS transition of QD. $M$ is the total number of QD groups in the sheet and is divided according to the full-width at half maximum of the spectrum. $M = 15$ is assumed which results in a system with 33 rate equations. $N_{GS}$ represents GS with transition energy closer to the lasing energy $E_j$. In Eq. (1), $\beta$ is the spontaneous emission factor, $\gamma$ is the feedback level ($\gamma = \sqrt{R_f}/\tau_{activ}$), $R_f$ is the external feedback level (the fraction of emitted power couple back to the laser). The round-trip time in the activ region is $\tau_{activ} = 2L/v_g$ with $L$ is the active region length and $v_g$ is the group velocity; $\tau_{delayed}$ is the round-trip delay time in the external cavity. The recombination time is $\tau_r$ and the photon life-time is $\tau_{pGS}$ taken at the ground state transition; $n_r$ is the refractive index of the QD, $c$ is the speed of light in free space, $\Gamma$ is the optical confinement factor of the active layer. $I$ is the injection current, $q$ is the elementary charge. The frequency fluctuations are calculated from the structure parameters with the inclusion of plasma effect, which has a considerable contribution. Plasma effects is not included in other models, see [3] for example. The fluctuation of laser frequency ($\delta w$) is given by [7]

$$\delta w(t, E_j) = -\frac{E_m}{2\pi\hbar n_g} \Delta n_{eff}(t, E_j). \qquad (6)$$

$\Delta n_{eff}$ is the total effective refractive index variation which have a plasma and QD contributions, ($\Delta n_{eff} = \Delta n_{QD}$

$+ \Delta n_{plasma}$). The plasma contribution is a sum of two terms: the term due to the free carrier accumulation in the two dimensional WL and three dimensional SCH layer, i.e.

$$\Delta n_{plasma} = \left[\Gamma_{SCH} \frac{N_s}{E_j^2} + \Gamma_{wl} \frac{N_{wl}}{E_j^2}\right] K_{plasma}$$

where

$$K_{plasma} = \frac{-\hbar^2 q^2}{2\varepsilon_0 n_r m_e^*}$$

and the term due to the QD gain variation, which is given by

$$\Delta n_{QD}(E_j) = \Gamma \frac{\hbar c}{2E_j} C_g N_D$$
$$\times \sum_k \sum_m \mu_k \frac{|P_k^\delta|^2}{E_k} (2P_{km} - 1) G_m D_{cv}(E_j - E_{km}).$$

Note that the homogenous broadening function of the refractive index spectrum is

$$D_{cv}(E_j - E_{km}) = \frac{(E_j - E_{km})/\pi}{(E_j - E_{km})^2 + (\hbar\Gamma_{hom})^2}.$$

In Eqs (2)–(4), the diffusion and recombination times in the barrier (SCH) layer are $\tau_s$ and $\tau_{sr}$, respectively. The average capture times from the WL to the ES is $\tau_{c0}$ and from the ES to the GS is $\tau_{d0}$ supposing that the final state is empty. The Pauli blocking terms for GS and ES are $(1 - P_{GSm})$ and $(1 - P_{ESm})$, respectively. $P_{GSm}$ and $P_{ESm}$ are the filling probability of the GS and ES, respectively. Pauli blocking terms for the escape from the WL to the SCH is neglected because we assume the WL and SCH states are always weekly occupied. Furthermore, at room temperature and without stimulated emission the system must converge to a quasi-thermal equilibrium characterized by a Fermy distribution of the carriers in all the states. To ensure this comvergence the carrier escape times are related to the carrier capture times by:

$$\tau_{eGSm} = \tau_{d0} \frac{\mu_{GS}}{\mu_{ES}} e^{([E_{ESm} - E_{GSm}]/k_B T)}$$

and

$$\tau_{eESm} = \tau_{c0} \frac{\mu_{ES}N_D}{\rho_{weff}} e^{([E_{wl} - E_{ES}]/k_B T)},$$

where $\tau_{eGSm}$ and $\tau_{eESm}$ are the escape times from the $m^{th}$ GS or ES, respectively. Note that $N_D$ is the density of QDs per unit area, $\mu_{GS} = 2$ and $\mu_{ES} = 4$ are the degeneracy of the GS and ES levels, respectively, including the spin. For the excape time from the WL in the SCH we use

$$\tau_{we} = \tau_s \frac{\rho_{weff}N_{QD}}{\rho_{SCH}H_b} \exp(\Delta E_{SCH,wl}/k_B T)$$

with $\rho_{weff}$ is the density of states per unit area in the WL and $\rho_{SCH}$ is the density of states per unit volume in the SCH. They are given by $\rho_{weff} = (m_{ewl}k_B T/\pi\hbar^2)$ and $\rho_{SCH} = 2(2m_{eSCH}\pi k_B T/\hbar^2)^{3/2}$. $N_{QD}$ is the number

Parameters for the quantum dot material and laser [6]

| QD material prameter | Laser parameter |
|---|---|
| Diffusion time in SCH $\tau_s = 6$ ps | Active region length $600\,\mu$m |
| SCH recombination time $\tau_{sr} = 4.5$ ns | SCH thickness $90$ nm |
| WL recombination time $\tau_{wr} = 3$ ns | WL thickness $1$ nm |
| Capture time from WL to ES $\tau_{c0} = 1$ ps | Active region width $10\,\mu$m |
| Capture time from ES to GS $\tau_{d0} = 7$ ps | Number of QD layers $3$ |
| ES and GS recombination time $\tau_r = 2.8$ ns | Active region volume $2.2 \cdot 10^{-16}$ m$^3$ |
| Energy separation SCH and WL $= 84$ meV | Density of QDs per layer $N_D = 6.3 \cdot 10^{22}$ m$^{-3}$ |
| Average energy separation WL and ES $= 100$ meV | SCH confinement factor $\Gamma_{\text{SCH}} = 0.1$ |
| Average energy separation ES and GS $= 80$ meV | WL confinement factor $\Gamma_{wl} = 0.1$ |
| Average recombination energy from GS $E_{GS0} = 0.96$ eV | QD optical confinement factor $\Gamma = 0.06$ |
| FWHM of homogeneous broadening $2\eta\Gamma_k = 20$ meV | Internal modal loss $\alpha = 0.7336$ cm$^{-1}$ |
| FWHM of inhomogeneous (Gaussian) broadening $40$ eV | Spontaneous emission factor $\beta = 10^{-4}$ |
| Number of QD sub-groups $M = 15$ | |

of QD layers and $H_b$ is the total thickness of the SCH. The laser is assumed here to be work at GS transition only (which is possible with the type of laser studied here, distributed Bragg reflector (DBR)). The contribution of various QD populations at the mode energy $E_j$ is also included. Therefore, gain for GS is written as [6]

$$g_{jm\text{GS}} = \mu_{\text{GS}} C_g N_D \frac{|P^{\sigma}_{\text{GS}}|^2}{E_{\text{GS}m}} (2P_{\text{GS}m} - 1) G_m B_{cv}(E_j - E_{\text{GS}m}),$$
(7)

where

$$C_g = \frac{\pi e^2}{n_b\, c\, \varepsilon_0 m_0^2 w_{\text{GS}m}^2},$$

with $w_{\text{GS}m}$ is the angular frequency at the $m^{th}$ ground state transition, $|P^{\sigma}_{\text{GS}}|^2$ is the transition matrix elements of the GS recombination, $G_m$ is the existence probability of the $m^{th}$ QD subgroup assuming that $\sum_m G_m = 1$ is satisfied, $B_{cv}(E - E_{\text{GS}})$ is the Lorentzian homogeneous broadening function with width $\hbar\Gamma_{\text{hom}}$.
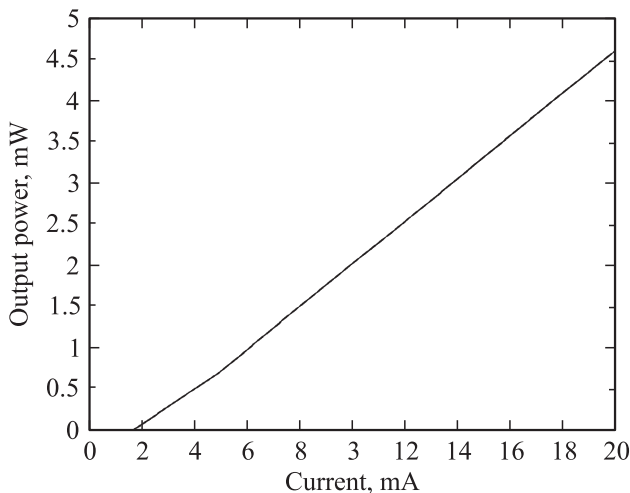


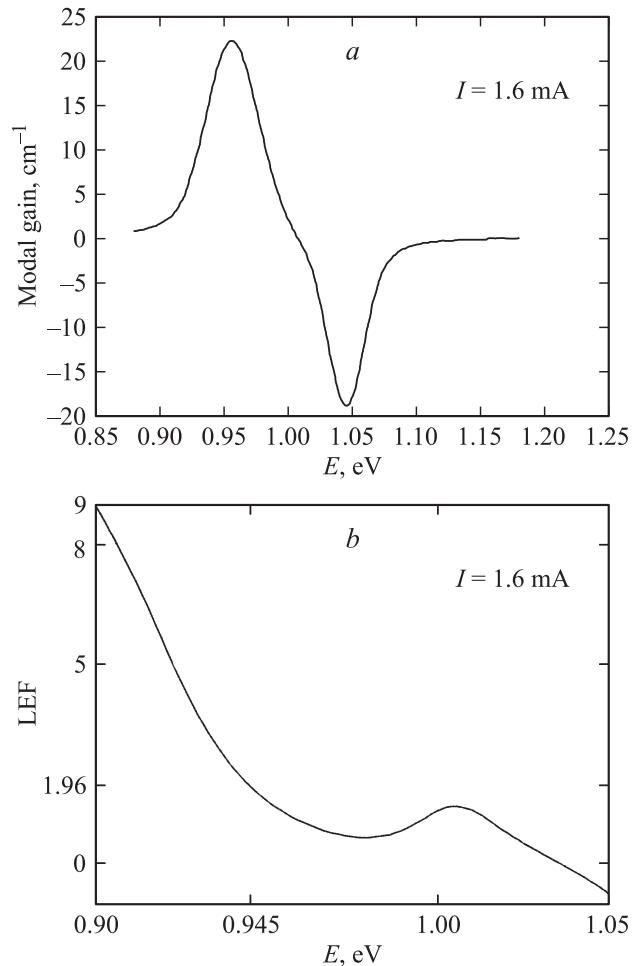**Figure 1.** Power–current characteristic for ground-state transition.



**Figure 2.** *a* — gain and *b* — linewidth enhancement factor (LEF) at threshold current of ground-state transition.

## 3.  Calculations and discussion

### 3.1.  Choice of the operating point

The simulation is done here for a DBR QD laser diode (LD). Table reports the parameters of the QD material
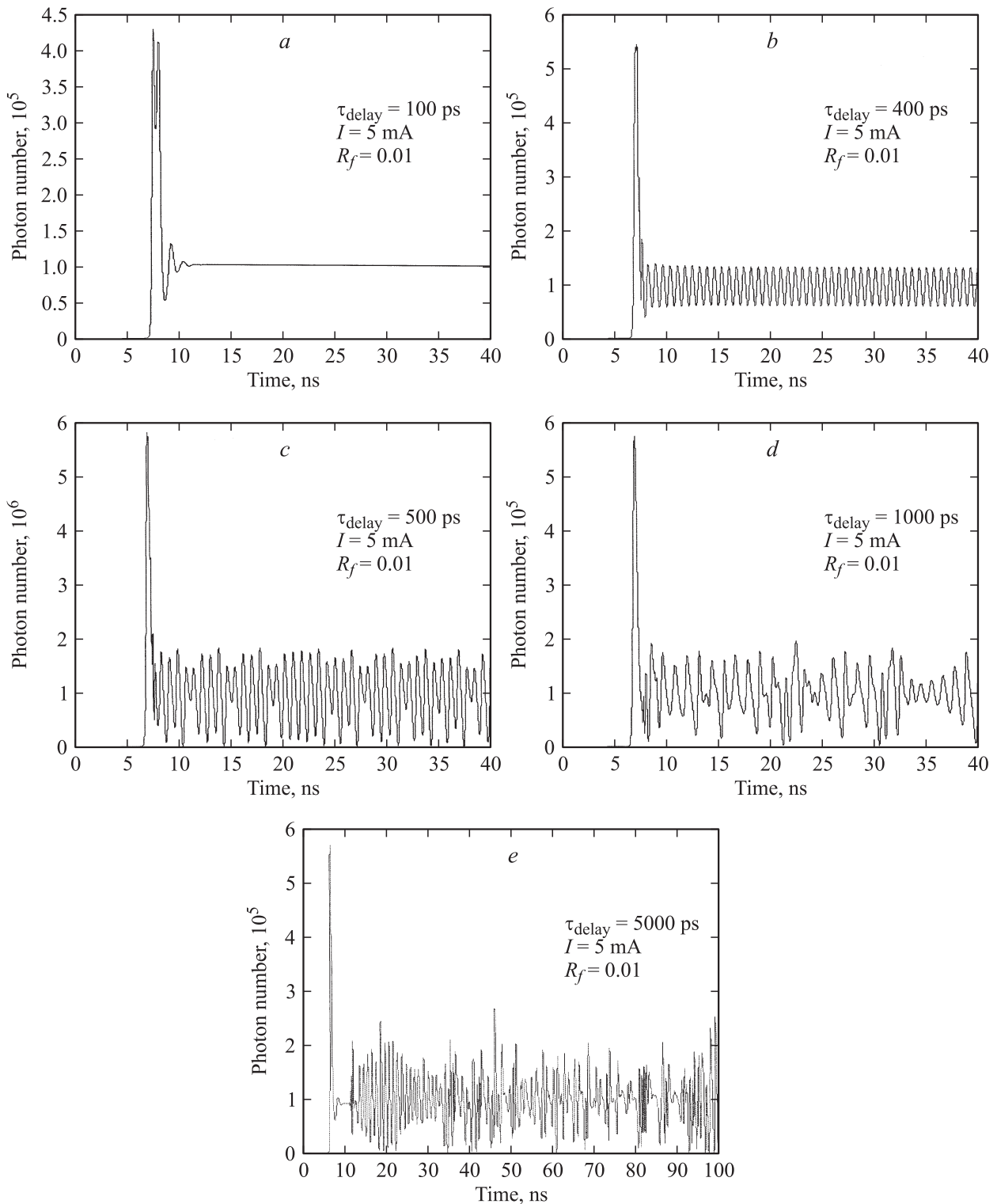
**Figure 3.** Temporal behavior for distributed Bragg reflector-laser diode at $I = 3.1I_{th}$ for: $a$ — $L_{ext} = 15\,mm$ ($\tau_{delayed} = 100\,ps$), $b$ — $L_{ext} = 60\,mm$ ($\tau_{delayed} = 400\,ps$), $c$ — $L_{ext} = 21\,mm$ ($\tau_{delayed} = 500\,ps$), $d$ — $L_{ext} = 42\,mm$ ($\tau_{delayed} = 1000\,ps$) and $e$ — $L_{ext} = 210\,mm$ ($\tau_{delayed} = 5000\,ps$). Note that $R_f = 0.01$.

under study. The QD material system chosen here is InAs–GaAs. To study feedback dynamics, we need first to specify the operating point that laser works on. So, power–current $(P-I)$ characteristic of this QD laser is shown in Fig. 1 where the threshold current for the GS transition is found to be 1.6 mA. A kink is shown at $\sim 5$ mA of the $P-I$ characteristics in Fig. 1. It is demonstrated experimentally that a kink appears near threshold due to
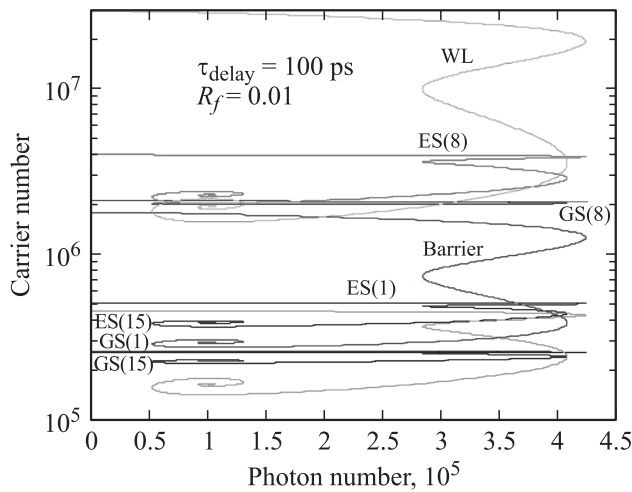
**Figure 4.** Phase portraits for distributed Bragg reflector-laserdiode with external cavity length $L_{\text{ext}} = 15\,\text{mm}$ ($\tau_{\text{delayed}} = 100\,\text{ps}$) at 5 mA for the barrier, WL, 1$^{\text{st}}$, 8$^{\text{th}}$ and 15$^{\text{th}}$ groups of the QD GS and ES.

feedback in semiconductor lasers [8]. Note that the kink cannot be explained by nonlinearity or multi-mode behavior. Nonlinearity is neglected here in the rate equations (REs) model as it is done by a most of the articles dealing with QD behavior. Including nonlinearity in the REs model of QDs is still as a work to be done in the near future. By using DBR the multi-mode behavior is neglected. Gain and LEF at these threshold values are shown in Fig. 2, *a* and *b*. It is shown that GS transition is taken at 0.957 eV, $\lambda = 1.31\,\mu\text{m}$ where we choose it as the operating point for DBR-LD studied here. For this DBR-LD operating point the LEF value is 1.96, see Fig. 2, *b*.

### 3.2. Feedback

Feedback is studied in DBR-LD at different external cavities and pumping currents. Fig. 3 shows the temporal behavior at 5 mA pumping current ($I = 3.1I_{\text{th}}$) and different external cavities. For an external cavity length $L_{\text{ext}} = 15\,\text{mm}$ ($\tau_{\text{delayed}} = 100\,\text{ps}$), Fig. 3, *a*, the laser delays (7 ns) before
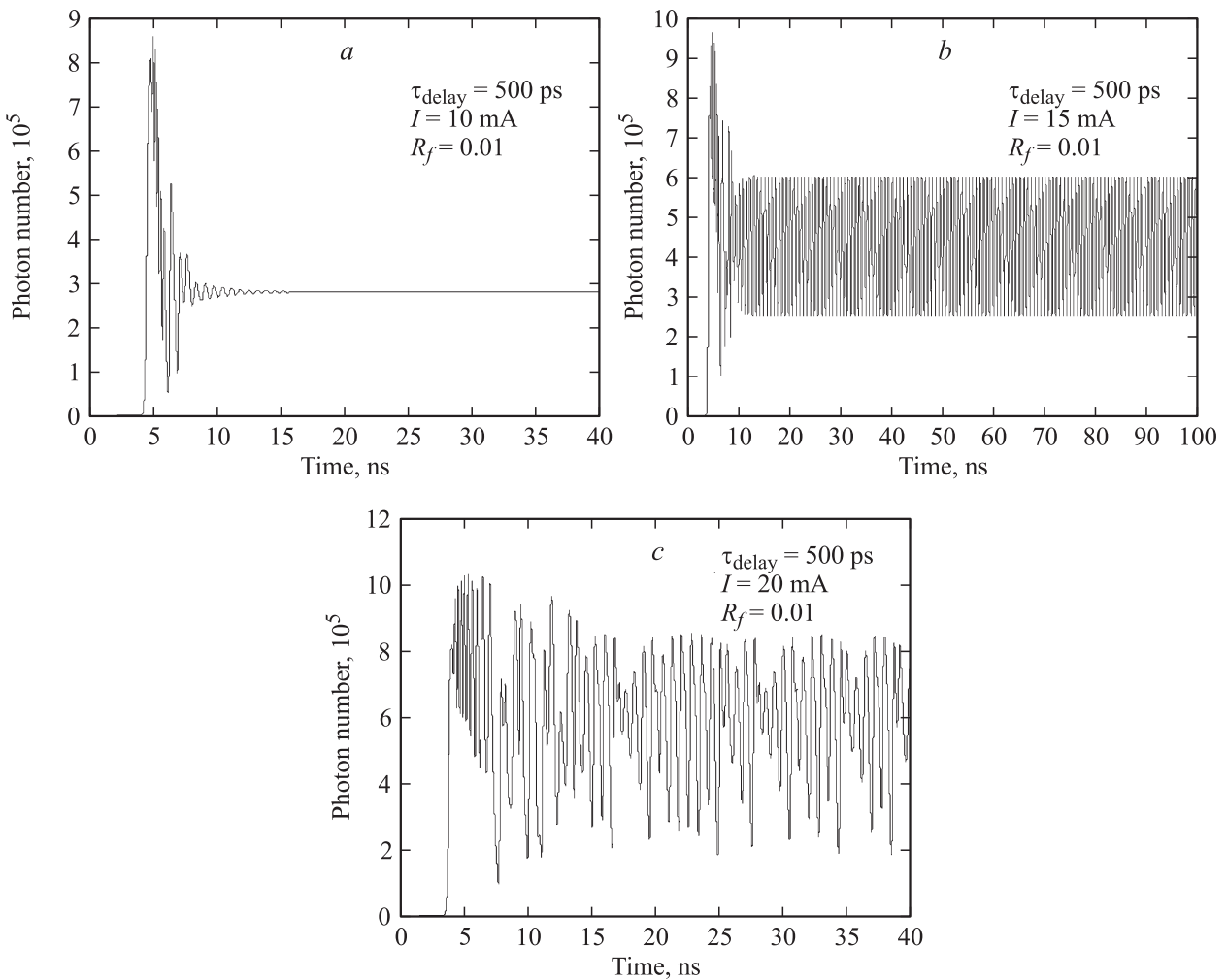


**Figure 5.** Temporal behavior for distributed Bragg reflector-laser diode with $L_{\text{ext}} = 75\,\text{mm}$ ($\tau_{\text{delayed}} = 500\,\text{ps}$), $R_f = 0.01$ at: *a* — $I = 6I_{\text{th}}$, *b* — $I = 9.7I_{\text{th}}$ and *c* — $I = 12.51I_{\text{th}}$.

the inversion takes place. After this, the oscillations are completely damped. When the external cavity length increases to $L_{ext} = 60$ mm ($\tau_{delayed} = 400$ ps), a periodic oscillations appear. The corresponding time series can be shown in Fig. 3, *b*. For longer external cavity, the time series shows the development of these oscillations to a periodic orders (doubling, tripling...) as in Fig. 3, *c, d*. At longer ones it developed to chaos as in Fig. 3, *e*, where an irregular pulse-like shape can be seen in the earlier periods of oscillation. The long external cavity is dominant since the relaxation oscillation frequency, and then the damping rate, is known to increase [1] with longer cavity length. In Fig. 4, projections of the trajectories onto the ($N_{ph}$, $N_{GS}$), ($N_{ph}$, $N_{ES}$), ($N_{ph}$, $N_{wl}$), ($N_{ph}$, $N_s$) planes show motions of stable limit cycle, where $N_{ph}$ is the photon number. Here we plot the states in the same $N_{ph}$-carrier number plane for comparison. For $L_{ext} = 15$ mm, no trace of relaxation oscillations is seen for all trajectories. To examine the effect of the injection current, Fig. 5 shows the spectra of DBR-LD at external cavity $L_{ext} = 75$ mm ($\tau_{delayed} = 500$ ps). At 10 mA ($I = 6I_{th}$), Fig. 5, *a*, a less sensitivity to feedback is obtained but at higher current value, 15 mA ($I = 9.7I_{th}$), feedback oscillations are attained, as in Fig. 5, *b*, and a lager amplitude of feedback oscillations is appear. With increasing current to 20 mA ($I = 12.5I_{th}$) the oscillations are developed from frequency periods to irregular pulse-like shape. This is seen in Fig. 5, *c*. The phase portraits of Fig. 5, *b* are displayed in Fig. 6 for WL, barrier layer states, QD GS and ES (1, 8 and 15 groups). While group 15th QD ES has an obvious contribution, the main contribution to feedback oscillations is shown to be comes from the WL which is work as a common reservoir. This observation coincides with earlier results [1] as the frequency fluctuation in QDs is controlled by LEF which have a plasma contribution comes from WL. The contribution of QD groups can only be followed with MPRE model since the simple RE models uses only one or two QD groups [9]. According to these figures, one cannot neglect the contribution of groups other than the resonant group (8th group here). This can view the importance of using MPRE in the QD simulation since all groups are contributes in the behavior. More view can be seen by plotting occupation probability for different QD groups of DBR-LD without feedback as seen in Fig. 7 where the main contributions are seen from the 1st GS group. This is also with main conclusion of [9] where the occupation probability of GS above that of the ES in QDs. A hole appears in the occupation probability curves. As we see earlier, the QDs are divided into groups depending on the homogenous broadening. So, there is an existence probability for each group [7]. These groups have different contributions to the QD response. Each group can be effected by another groups. This behaviour can be represented by a wave propagation which can be accompanied by carrier depletion in this group. This behavior is not shown with ordinary RE models. But it can be shown when a pulse „Gaussian" is applied to the system [9]. Curves arrangement in Fig. 7
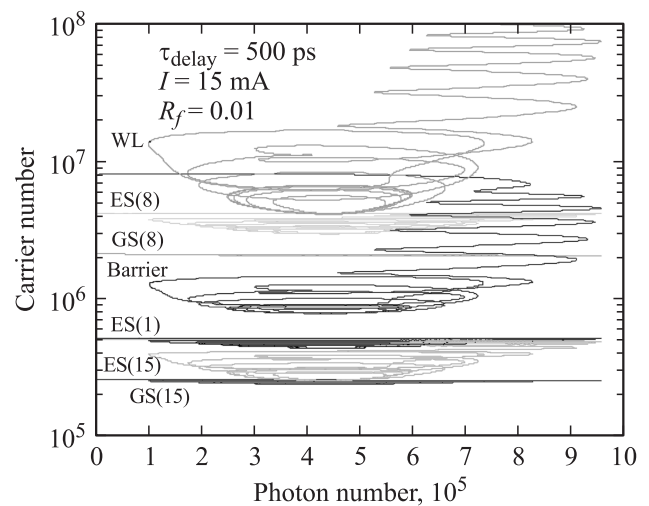
**Figure 6.** Phase portraits for distributed Bragg reflector-laser diode with external cavity length $L_{ext} = 75$ mm ($\tau_{delayed} = 500$ ps) at 15 mA for the barrier, wetting layer, 1st, 8th, and 15th groups of the quantum dot ground- and exited states. The 1st ground states group of quantum dot disappears since it is completely under the 15th ground states group.
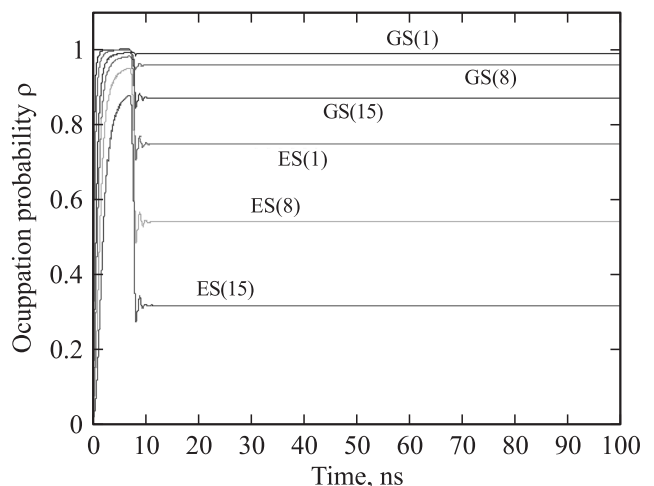


**Figure 7.** Temporal behavior for the 1st, 8th and 15th occupation probabilities of ground and exited states groups of distributed Bragg reflector-laser diode.

depends on the escape times $\tau_{eGSm}$ and $\tau_{eESm}$ of the groups where the state with longer time gets occupation higher than the latter. For example, GS(1) group with an escape time ($\tau_{eGS1} = 0.116$ ns) have occupation probability higher than GS(8) group ($\tau_{eGS8} = 0.0773$ ns) while ES(15) group have the lowest occupation probability due to its shorter escape time ($\tau_{eGS15} = 0.00876$ ns). This can explains why the SRE models, which uses a single group to represents QDs, success in elucidate experimental observations. This is because most of RE models takes GS as the lasing states. While the difference between the 1st and last QD groups in the GS is too much, according to Fig. 7, these groups
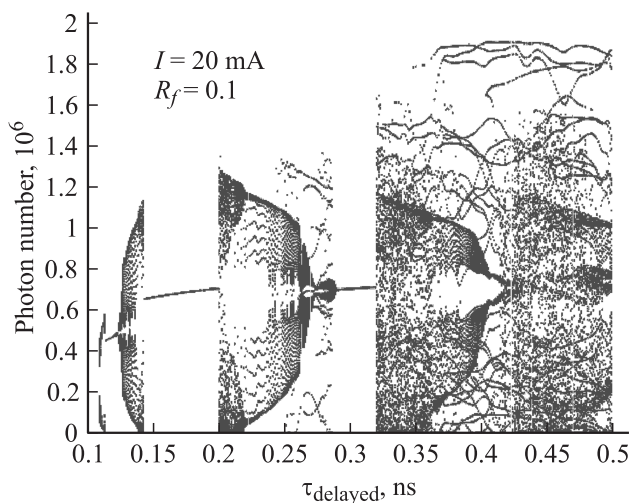
**Figure 8.** Bifurcation diagram for distributed Bragg reflector-laser diode at higher feedback level ($R_f = 0.1$) and 20 mA current.

have observable difference for ES case — their occupation probabilities differ by $\sim 0.4$. So, one can expect simple RE model fails in explaining the behavior of a QD laser works at ES.

One can also refers to the turn-on delay time seen in Fig. 3 at $I = 3.1 I_{th}$, ($I = 5$ mA) which equals 6.5 ns while in Fig. 5,*a* at $I = 6 I_{th}$ (10 mA) it is 4 ns, in Fig. 5,*b* $I = 9.7 I_{th}$ (15 mA) it is 3.5 ns and in Fig. 5,*c* $I = 12.5 I_{th}$ (20 mA) it is 3.4 ns. Thus, the turn-on delay time is reduced with increasing current. The turn-on delay is the time needed to reach threshold which is important for laser performance. Our results demonstrates the inverse relation between turn-on delay with pumping current which is also fulfilled theoretically and experimentally in [10]. It is found that the turn-on delay time is reduced with higher optical confinement factor or gain [11]. Since optical confinement factor is constant in our simulation, so the factor affecting here is the gain which increases with injection current, thus reduces the turn-on time.

Finally we plot the bifurcation diagram for DBR-LD at higher feedback level ($R_f = 0.1$) and 20 mA current for different external cavity lengths as seen in Fig. 8. This figure shows the chaotic behavior at longer external cavity ($\geq 350$ ps). Because the bifurcation diagram in Fig. 8 is done along range of external cavity time ($\tau_{delayed}$) and obtained using a long integration time period, so it can contain also points from the beginning of oscillations where the photon density is high. The chaotic behavior in Fig. 8 is expected since it is well known that [12] as the feedback level increased, a sequence of periodic oscillations was observed at increasing multiples of the round-trip frequency until the chaotic behavior is appear. This is probably related [1] to multiple lasing modes in the experiment which is not taken in MPRE system here.

## 4. Conclusions

We proposed a model based on the MPRE to simulate feedback in QD lasers. The model illustrates the behavior in the form of feedback oscillations, periodic oscillations and the chaos at higher feedback levels. It is shown that feedback oscillations reasoned mainly to WL states. The model shows the contribution of QD groups in the oscillations and expects that because of the observable differences between QD groups in the excited state the simple rate equation models cannot explain the behavior of a QD laser working at excited state transition.

## References

[1] E.A. Viktorov, P. Mandel, G. Huyet. Optics Lett., **32**, 1268 (2007).

[2] E.A. Viktorov, P. Mandel, I. O'Driscoll, O. Carroll, G. Huyet, J. Houlihan, Y. Tanguy. Optics Lett., **31**, 2302 (2006).

[3] D. O'Brien, S.P. Hegarty, G. Huyet, A.V. Uskov. Optics Lett., **29**, 1072 (2004).

[4] W.L. Zhang, W. Pan, B. Luo, X.H. Zou, M.Y. Wang. IEEE Photon. Technol. Lett., **20**, 712 (2008).

[5] R. Lang, L. Kobayashi. IEEE J. Quant. Electron., QE-16, 347 (1980).

[6] M. Gopannini, A. Sevega, I. Montrosset. Opt. Quant. Electron., **38**, 381 (2006).

[7] M. Gioannini, I. Montrosset. IEEE J. Quant. Electron., **43**, 941 (2007).

[8] J. Mork. Report No. S48, The Danish center for applied mathematics and mechanics, Technical University of Denmark, Denmark, March 1989.

[9] Y. Ben Ezra, B.I. Lembrikov, M. Haridim. IEEE J. Quant. Electron., **41**, 1268 (2005).

[10] K. Ludge, M. Bormann, E. Malic, P. Hovel, M. Kuntz, D. Bimberg, A. Knorr, E. Scholl. Phys. Rev. B, **78**, 035 316 (2008).

[11] K. Lüdge, E. Scholl. IEEE J. Quant. Electron., **45**, 1394 (2009).

[12] O. Carroll, I. O'Driscoll, S.P. Hegarty, G. Huyet, J. Houlihan, E.A. Viktorov, P. Mandel. Opt. Express, **14**, 10 831 (2006).